

1 **Activated Sludge Model 2d calibration with full-scale WWTP data: comparing**
2 **model parameter identifiability with influent and operational uncertainty.**

3

4 Vinicius Cunha Machado, Javier Lafuente, Juan Antonio Baeza*

5

6 Department of Chemical Engineering, Universitat Autònoma de Barcelona, ETSE,

7 08193 Bellaterra (Barcelona), Spain. Phone: +34935811587. FAX: +34935812013.

8 E-mails: vinicius.cunhamachado@gmail.com, javier.lafuente@uab.cat,

9 juanantonio.baeza@uab.cat

10

11 *Corresponding Author

12

Post-print of: Cunha, V; Lafuente, FJ and Baeza, JA "Activated sludge model 2d calibration with full-scale WWTP data: comparint model parameter identifiability with influent and operational uncertainty" in Bioprocess and biosystems engineering (Ed. Springer), vol. 37, issue 7 (July 2014), p. 1271-1287. The final versión is available at DOI 10.1007/s00449-013-1099-8

13 **Abstract**

14 The present work developed a model for the description of a full-scale WWTP
15 (Manresa, Catalonia, Spain) for further plant upgrades based on the systematic
16 parameter calibration of the ASM2d model using a methodology based on the Fisher
17 Information Matrix (FIM). The influent was characterized for the application of the
18 ASM2d and the confidence interval of the calibrated parameters was also assessed. No
19 expert knowledge was necessary for model calibration and a huge available plant
20 database was converted into more useful information. The effect of the influent and
21 operating variables on the model fit was also studied using these variables as calibrating
22 parameters and keeping the ASM2d kinetic and stoichiometric parameters, which
23 traditionally are the calibration parameters, at their default values. Such an “inversion”
24 of the traditional way of model fitting allowed evaluating the sensitivity of the main
25 model outputs regarding to the influent and to the operating variables changes. This new
26 approach is able to evaluate the capacity of the operational variables used by the WWTP
27 feedback control loops to overcome external disturbances in the influent and
28 kinetic/stoichiometric model parameters uncertainties. In addition, the study of the
29 influence of operating variables on the model outputs provides useful information to
30 select input and output variables in decentralized control structures.

31

32 **Keywords:** ASM2d, EBPR, FIM, full-scale WWTP, calibration, influent
33 characterization, modelling.

34

35

36 **Nomenclature**

37 A²/O Anaerobic, Anoxic and Aerobic (WWTP configuration)

38 ASM Activated Sludge Models

39 BOD₅ Biological Oxygen Demand (5 days)

40 CCF Calibration Cost Function

41 COD Chemical Oxygen Demand

42 DO Dissolved Oxygen

43 EBPR Enhanced Biological Phosphorus Removal

44 FIM Fisher Information Matrix

45 GAO Glycogen Accumulating Organisms

46 IWA International Water Association

47 PAO Phosphorus Accumulating Organisms

48 PCCF Preliminary Calibration Cost Function

49 PID Proportional-Integral-Derivative controller

50 SRT Sludge Retention Time

51 TKN Total Kjeldahl Nitrogen

52 TN Total Nitrogen

53 TSS Total Suspended Solids

54 VCF Validation Cost Function

55 WWTP Wastewater Treatment Plant

56 WERF Water Environment Research Foundation

57

58 **1. Introduction**

59 Modelling wastewater treatment plants (WWTP) is the fundamental stone to improve
60 WWTP performance through identifying bottlenecks and proposing modifications of
61 existent plants or to design a completely new one. Besides the experimental knowledge,
62 mathematical models are a set of tools for predicting plant behaviour under different
63 conditions from the ordinary outlook of the WWTP or under unexpected operational
64 scenarios [1]. The models are also useful for changing process concepts and developing
65 new plant configurations [2]. The operation of WWTPs is based on the behaviour of
66 different microorganisms, which are responsible for biological nutrient (nitrogen and
67 phosphorus) and organic matter (carbon) removal. Such processes are well described by
68 the IWA models ASM1, ASM2, ASM2d and ASM3, even though other models have
69 been used and accepted in practical and scientific media as the TUD-P model [3–5] or
70 the ASM3 EAWAG Bio-P [6]. ASM2d model is being used in many researches
71 concerning WWTP due to including the most important biological processes of ordinary
72 heterotrophic biomass, heterotrophic PAO biomass and nitrifiers. Ferrer et al. [7] used
73 this model to fit full-scale WWTP data and then to evaluate different configurations for
74 improving nutrient removal. Ingildsen et al. [8] calibrated the ASM2d model for the
75 Avedøre WWTP (Denmark) to support a control strategy for maintaining the enhanced
76 biological phosphorus removal (EBPR) process activated for long periods. Xie et al. [9]
77 also used ASM2d to simulate and optimize a full-scale Carrousel WWTP. García-Usach
78 et al. [10] or Machado et al. [11] successfully used ASM2d for describing EBPR
79 process at pilot scale.

80 WWTP models are also useful for studying and proposing several control strategies in
81 order to guarantee the effluent quality with or without external disturbances (storm
82 events, peaks of pollutants in the influent...). The effluent quality is the main goal of the

83 control structures, where ammonium, nitrate and phosphorus are the main pollutants
84 that should be kept at lower values to avoid the eutrophication effect. Nevertheless,
85 dissolved oxygen (DO) and the sludge residence time (SRT) are the inventory variables
86 that should be controlled first [12]. To control ammonium concentration, a cascade
87 controller which calculates the DO setpoint in the aerobic basin using the error between
88 the desired ammonium concentration and the real measurement in the effluent is
89 designed [13]. An ammonium feedback-feedforward controller also could be
90 implemented if the ammonium influent load is estimated or measured [14]. Nitrate
91 removal is accomplished by the denitrification processes which depend on the readily
92 organic matter available in an anoxic zone and the nitrate concentration. Two ways of
93 controlling the nitrate concentration at the effluent is adding external carbon source and
94 changing the nitrate recycle from the aerobic basin to the anoxic one in most of WWTP
95 [15, 16]. It is worth noticing that the measured and the manipulated variables also have
96 uncertainties, like recycling flow measurements and dissolved oxygen concentrations.
97 All the abovementioned control applications using WWTP models should be preceded
98 by a correlation analysis of the available manipulated variables not to add internal
99 disturbances to control the effluent quality.

100 Despite all the cited models are essential tools for improving many aspects of the
101 wastewater treatment, they are structured on kinetic and stoichiometric parameters that
102 should be identified for better accuracy. Besides, their state variables are not exactly the
103 same as the information obtained from laboratory analysis periodically performed in the
104 WWTP. Therefore, it is necessary, first, to convert some daily plant measurements of
105 the influent into model states and, second, to calibrate parameters using plant data and
106 lab assays (batch tests with the plant biomass). In the literature it is possible to find a
107 methodology to accomplish the first task before mentioned [17], although the influent

108 identifiability linked to its variability has not received much attention. The parameter
109 calibration could be performed using protocols reported in the literature [18, 19] as the
110 protocols developed by STOWA [20], BIOMATH [21], WERF [22], HSG [23] or
111 Mannina et al. [24, 25]. All these protocols are good at posing well the goals of the
112 calibration, systematically treat the plant data gathered and have a validation step with
113 different data from those used to calibrate the model. On the other hand, only
114 BIOMATH, WERF or Mannina et al. protocols pay attention to the parameter subset
115 selection to maximize the information mined from the plant data. Machado et al. [11],
116 developed an alternative calibration methodology, called the “seeds methodology”,
117 using criteria derived from the Fisher Information Matrix (FIM) to avoid overfitting.
118 Although the hydraulics modelling and a detailed biomass characterization are not
119 emphasized in this last method as in the HSG and BIOMATH protocols, respectively,
120 the usage of a large amount of available plant data combined with a systematic
121 procedure to find the most identifiable parameters subset, without testing all the
122 possible parameters combinations, are the strengths of the “seeds methodology”.
123 Unfortunately, the performance of all the abovementioned protocols is affected by
124 uncertainties from different sources during the modelling task. Refsgaard et al. [26]
125 pointed out that several error sources affect the quality of model simulation results: (i)
126 context and framing; (ii) input uncertainty; (iii) model structure uncertainty; (iv)
127 parameter uncertainty and (v) model technical uncertainty. Sin et al. [27] deepened in
128 the uncertainty analysis, concluding that both biokinetic/stoichiometric/influent
129 fractionation related parameters as well as hydraulics/mass transfer related parameters
130 induced significant uncertainty in the predicted performance of WWTP. Moreover,
131 Cierkens et al. [28] studied the effect of the influent data frequency on the calibration
132 quality and output uncertainty of the WWTP model fit.

133 Uncertainty assessment of kinetic and stoichiometric model parameters of ASM1 and
134 ASM2 has been applied for full-scale WWTP as in Mannina et al. [29], who evaluated
135 the model reliability identifying the crucial aspects where higher uncertainty rely and
136 more efforts should be provided in terms of both data gathering and modelling practises.
137 The uncertainty associated to operation and design parameters of WWTP have also been
138 studied [30] showing that they are the most sensitive parameters for some
139 benchmarking studies. Finally, Belia et al. [31] pointed out that identifying and
140 quantifying the uncertainties involved in a new design or plant upgrade becomes crucial
141 because WWTP are required to operate with increased energy efficiency and close to
142 their limits. They also note the need for the development of a protocol to include
143 uncertainty evaluations in model-based design and optimisation projects.

144 To consider some kind of those commented uncertainties on the modelling task and
145 concentrating effort at the calibration step, the present work developed an AS model for
146 the Manresa WWTP (Manresa, Catalonia, Spain) based on the systematic parameter
147 calibration of the ASM2d model using the “seeds methodology” for further plant
148 upgrades, as the insertion of the EBPR and the design of a new control structure for the
149 plant. The influent was characterized as required by the ASM2d and the parameters
150 were selected, calibrated and their confidence intervals were assessed as stated in the
151 “seeds methodology”. The calibration parameters were divided into three groups: the
152 traditional kinetic/stoichiometric parameter group (K group); the influent factors
153 representing errors/uncertainties of the influent characterization (I group) and the
154 operational variable factors (O group), considering errors/uncertainties on the
155 measurement of the operational variables. The procedure assessed, in addition to the
156 conventional calibration of the K group, influent and operational variables uncertainties
157 in two additional calibrations: i) influent vector of states in the ASM2d model (I group)

158 was used as calibration parameters while parameters of K and O groups were kept at
159 their default values and ii) the O group was used as calibrating parameters while K and I
160 groups kept constant. Such “inversion” of the traditional model fit procedure allowed to
161 evaluate the quality of the influent characterization and to observe the set of operating
162 variables which has the less number of uncorrelated variables amongst themselves for
163 better designing a decentralized control structure for the WWTP.

164

165 **2. Material and Methods**

166 **2.1 Brief description of the Manresa WWTP**

167 The average flow rate of Manresa WWTP is 27,000 m³/d. This WWTP (Figure 1)
168 consists of a pre-treatment (gross and grit removal), primary treatment with a clarifier, a
169 secondary stage (biological removal) and a possible tertiary stage (chlorination). There
170 are two main treatment lines in the secondary stage (Figure 2). Each line has three
171 anoxic reactors (1460 m³) and one aerobic reactor made up by two parts of 3391 m³.
172 Each reactor has approximately 7 m of depth. After passing through the anoxic zone, the
173 bulk liquid is mixed and is again divided to feed the aerobic zone. Air is bubbled from
174 the bottom of the aerobic tanks with membrane diffusers, allowing biological oxidation
175 of the organic matter and ammonium. An internal recycle pipe connects the aerobic
176 zone to the anoxic one in order to bring the nitrate to be denitrified in the anoxic zone.
177 At the end of the secondary stage two settlers separate the biomass from the treated
178 effluent. Settled biomass returns to the entrance of the anoxic reactor by an Archimedes
179 screw. The excess of sludge is anaerobically digested and sent to a composting plant.
180 The effluent, after leaving the secondary settler, can be chlorinated and it is disposed to
181 the environment at the Cardener River.

182 It is worth noticing that experimentally is observed preferential flux of the inlet mass
183 stream to one of the main treatment lines. The presence of DO (0.5-1.0 mg/L) at the end
184 of the anoxic reactors indicates that the denitrification is not occurring at the maximum
185 intensity because there is a lack of organic matter to improve the nitrate reduction and a
186 poor mixing is taking place. Also, a non-homogeneous spatial distribution of DO was
187 observed along the aerobic reactors, not only along the influent path but also in depth.
188 Daily analyses of COD, BOD5, total suspended solids (TSS), NH_4^+ , NO_3^- , PO_4^{3-} , total
189 Kjeldahl nitrogen (TKN) and total nitrogen (TN) are performed at the influent and the
190 effluent of the secondary treatment. The daily composite samples are collected from the
191 full-scale WWTP by sampling every 2 hours. The only system variable measured in
192 each reactor of the secondary treatment is the TSS concentration. .

193 The air supply system is composed by 4 air blowers with 100,000 Nm^3/d of capacity,
194 whose motor speed are controlled by a single DO feedback controller in the aerobic
195 basins. The aerobic zone of each water line has two on-line DO sensors, one of them
196 placed at the 25% of the path along the zone and the other one placed at 75% of the
197 aerobic zone. The DO PI controller uses a weighted average of the four DO
198 concentrations as the measured variable, and compares it to a DO setpoint, usually equal
199 to 2.0 mg/L. Once computed the error between the setpoint and the averaged DO, the
200 new setpoint speed of the blowers is calculated by the PI algorithm and sent to the
201 devices. Physically, the air is moved to a primary header after being discharged by the
202 blowers. Then, the air flow rate is divided into two branches. The right branch feeds the
203 middle part of the two aerobic zones while the left branch feeds the entrance and the end
204 of the two aerobic zones.

205 The main operation costs are electrical energy for aeration and pumping, sludge
206 treatment (anaerobic digestion and composting) and chemical products for P
207 precipitation.

208

209 **2.2 Influent composition and patterns**

210 Influent composition and its variability is key information for plant modelling and
211 description of changes along the year due to seasonal patterns. Table 1 shows influent
212 properties (averages) straightforward linked to the wastewater composition in winter
213 and summer months for the Manresa WWTP. Considering the effluent limits of COD
214 (125 mg O₂/L), BOD₅ (25 mg O₂/L), total N (10 mg/L), ammonium (4 mg/L) and total
215 P (1 mg/L), defined by the local water agency (Agència Catalana de l'Aigua, ACA), the
216 Manresa WWTP, with average effluent flow rate of 27,000 m³/day, could deliver an
217 effluent load of 3375 kg/d, 675 kg/d, 270 kg/d, 108 kg/d and 27 kg/d, respectively for
218 these pollutants. The total P discharge load was kept at the limit of 27 kg/d, which
219 means an average value of 1 mg/L of P, with large usage of FeCl₃ in 2008, 2009 and
220 2010. Such chemical precipitation represents a cost around 50,000 €/y, but allows
221 meeting the legal discharge level of the EC directive.

222 On summer months, contaminant loads are considerably lower than in winter months,
223 probably also due to the people moves from Manresa to vacation locations. These
224 qualitatively recognized patterns can be mathematically analysed looking for daily,
225 weekly or monthly profiles that could help to improve the tuning of feed-forward
226 controllers, for refusing external variations whose pure feedback controllers do not deal
227 easily, as well as to promote a time-scheduling load profile for dosing extra COD source
228 for denitrification and FeCl₃ for chemical P removal.

229

230 **2.3 Model structure**

231 The kinetic model implemented for modelling COD, N and P removal was the IWA
232 ASM2d model [5]. It has 19 state variables and 21 processes, which include nitrification
233 and denitrification and the PHA (poly-hydroxyalkanoates) accumulation process, the
234 latter fundamental for EBPR.

235 The settler model adopted was the 10 layer Takács model [32]. The wastewater entrance
236 is at the fifth layer. At the end of the process, the effluent leaves the settler from the
237 upper part (the collector, layer 1) and the settled biomass is recycled from the bottom of
238 the settler (layer 10) to the feed of the biological treatment. The recycled biomass
239 (external recycle, Q_{RAS}) is reincorporated to the process, being mixed to new influent of
240 the biological treatment. The soluble components of the wastewater leave the settler
241 with a concentration calculated considering CSTR behaviour for these compounds. The
242 settleability of particulate states is linked to the settling velocity which is calculated by a
243 double exponential function (Equation 1).

$$244 \quad v_s = v_0 \cdot e^{-r_h(X_i - f_{ns} \cdot X_{IN})} - v_0 \cdot e^{-r_p(X_i - f_{ns} \cdot X_{IN})} \quad \text{Eq. 1}$$

245 Where:

246 v_0 is the settling velocity if the *Stokes' Law* could be applied to the wastewater, [m/h];

247 f_{ns} is the fraction of non-settleable solids;

248 X_{IN} is the inlet solid concentration, [g TSS/m³];

249 X_i is the solid concentration of the layer i , [g TSS/m³];

250 r_h and r_p are weights for modelling the effect of the size of the particles in the settling
251 velocity.

252 Parameter v_s is compared to a maximum settling velocity, $v_{s,max}$, which is experimentally
253 determined. Xt is another model parameter required as a threshold value that indicates

254 an upper limit in the settler capacity to prevent an overflow of solids in the equipment.

255 The default values of the adopted model were:

$$\begin{array}{llll} v_0: & 500 \text{ m/h} & r_p: & 2.86 \cdot 10^{-3} & f_{ns}: & 2.28 \cdot 10^{-3} \\ v_{smax}: & 250 \text{ m/h} & r_h: & 5.76 \cdot 10^{-4} & X_t: & 3000 \text{ g TSS/m}^3 \end{array}$$

256

257 **2.4 Influent characterization according to the model states**

258 Although daily analysis of the influent is performed as detailed in section 2.1, additional
259 experimental data was needed to obtain the specific characterization required for
260 ASM2d. Therefore, some experiments were performed with wastewater leaving the
261 primary clarifier following the methodology described by Orhon et al. [33] as detailed
262 in Montpart [34]. The determined influent stream characteristics were $S_I = 0.080$ COD,
263 $X_I = 0.055$ COD, $X_S = 0.450$ COD and $S_F = 0.410$ COD and these ratios were assumed
264 constant. See supplementary information S1 for details of this characterization.

265 The values of the influent variables X_{TSS} , S_{NH4} , S_{NO3} , S_{PO4} were assumed to be equal to
266 the experimental observations (analysis of daily composite samples). The variables S_A ,
267 X_{PHA} , X_{PAO} , X_{PP} , S_{N2} , S_{O2} , X_A , X_{MEP} were assumed to be zero. Hence, the inlet
268 heterotrophic biomass was calculated by Equation 2:

$$269 \quad X_H = COD - (S_I + S_A + S_F + X_I + X_S + X_A) \quad \text{Eq. 2}$$

270 The variable X_{MEOH} was not considered zero due to the presence of chemical
271 phosphorus precipitant agent and its value along the time was defined in the steady state
272 calibration, when the phosphorus behaviour in the effluent was evaluated. Finally, S_{ALK}
273 (the plant influent alkalinity) was assumed to be 7 moles of $\text{HCO}_3^-/\text{m}^3$.

274

275 **3. Results and Discussion**

276 **3.1 Preliminary steady-state calibration**

277 Model calibration was performed in two steps: a steady-state calibration and a dynamic
 278 calibration. The former step was useful to minimize structural discrepancies between the
 279 plant model and plant data. By its turn, the dynamic calibration involved not only the
 280 determination of kinetic and stoichiometric parameters, but also an estimative of the
 281 useful volumes of reactors and settlers and the necessities of P chemical precipitant
 282 agent and extra load of biodegradable COD required for denitrification. Figure 3 shows
 283 a simplified scheme of the overall calibration / validation process used in this work.
 284 Preliminary calibration aims to reduce structural discrepancies between the model and
 285 the experimental variables, especially to reduce the main differences between
 286 experimental TSS and TSS model predictions. Experimental data were averaged
 287 (influent values and operational parameters like DO and flow rates) and the resultant
 288 values were used as inputs to the simulation model (constant inputs). A period of 1200
 289 days was simulated with the default ASM2d parameters and the steady-state values
 290 were used as initial values for all the simulations performed afterwards. TSS
 291 concentrations in the effluent and in the wastage purge stream were used as output
 292 variables to calibrate the following parameters:

- 293 a) r_p and f_{ns} (settling model parameters), to decrease the differences between TSS
 294 in the effluent and the model predictions for this output.
- 295 b) f_{Qw} and f_{QRAS} , in order to adjust the model TSS in the effluent and in the purge
 296 (and consequently in the solids inside the aerobic reactors).

297 A preliminary calibration cost function (PCCF, Equation 3) was employed to perform
 298 the preliminary steady-state calibration of the WWTP model.

$$299 \quad PCCF = \sum_{k=1}^2 q_k \sqrt{\sum_{r=1}^m (y_{Exp\ k,r} - y_{Model\ k,r})^2} \quad \text{Eq. 3}$$

300

301 Where:

- 302 • k is related to each output variable
- 303 • r is related to each experimental data (each day). The whole period studied had
- 304 $m = 1200$ days.
- 305 • q_k is the weight to normalize the output variables since their values are very
- 306 different. Ammonium was used as the reference value for the normalization, and
- 307 hence the weights were calculated as the ratio of the average of ammonium
- 308 concentration at the effluent to the average of the other output variable (TSS in
- 309 the effluent and in the external recycle) as shown in equation 4. The weights
- 310 used for the TSS in the effluent and in the external recycle were, respectively,
- 311 $3.637 \cdot 10^{-4}$ and $2.404 \cdot 10^{-4}$.
- 312 • $y_{Exp\ k,r}$ is the experimental data of variable k at day r .
- 313 • $y_{Model\ k,r}$ is the model output of variable k at day r .

314
$$q_k = \frac{\frac{1}{m} \sum_{r=1}^m y_{NH_4,r}}{\frac{1}{m} \sum_{r=1}^m y_{k,r}} \quad \text{Eq. 4}$$

315 Where $y_{k,r}$ is the data of the other output variables ($i = X_{TSS}$ at the effluent and X_{TSS} at

316 the purge) and m is the total number of experimental data ($m = 1200$).

317

318 In addition, X_{MeOH} in the influent was manipulated to adjust the phosphate

319 concentrations in the effluent. The calibrated values of the parameters were: $r_p =$

320 $1.036 \cdot 10^{-2}$, $f_{ns} = 2.566 \cdot 10^{-3}$, $f_{Q_w} = 0.1736$, $f_{QRAS} = 1.911$ and $f_{X_{MeOH}} = 1.237$. These

321 calibrated parameters were considered constant and were maintained in these values

322 during the dynamic calibration procedure. The values of the calibrated parameters f_{Q_w}

323 and f_{QRAS} were also used as initial guesses in the dynamic calibration of the Operational

324 Variables group

325

326 **3.2 Development of the cost function for dynamic calibration**

327 Data from seven effluent variables were available for model calibration of Manresa
328 WWTP: ammonium, nitrate, phosphorus, TSS, COD, BOD5 and TKN. These variables
329 were considered the output variables of interest. Data period used for model calibration
330 was from October 2007 to May 2008. Due to its daily oscillation, COD and BOD5 were
331 used only for model validation. In the dynamic calibration step, equation 5 was used as
332 cost function.

333

$$334 \quad CCF = \sum_{i=1}^5 w_i \sqrt{\sum_{j=1}^n (y_{Exp\ i,j} - y_{Model\ i,j})^2} \quad \text{Eq. 5}$$

335

336 Where:

- 337 • i is related to each output variable
- 338 • j is related to each experimental data (each day). The whole period studied had
339 $n = 251$ days.
- 340 • w_i is like q_k a weight to normalize all the output variables, which have different
341 units and values, using ammonium ($w = 1$) as a common base. Hence, the
342 weights were calculated as the ratio of the average of ammonium concentration
343 at the effluent to the average of the other output variable (NO_3^- , PO_4^{3-} , TSS and
344 TKN) as shown in equation 6. The weights calculated for nitrate, phosphorus,
345 TSS and TKN were 0.235, 1.124, 0.091 and 0.532, respectively.
- 346 • $y_{Exp\ i,j}$ is the experimental data of variable i at day j .
- 347 • $y_{Model\ i,j}$ is the model output of variable i at day j .

$$w_i = \frac{\frac{1}{n} \sum_{j=1}^n y_{NH_4, j}}{\frac{1}{n} \sum_{j=1}^n y_{i, j}} \quad \text{Eq. 6}$$

349 Where $y_{i,j}$ is the data of the other output variables ($i = \text{NO}_3^-$, X_{TSS} , N_{TKN} or PO_4^{3-}) and n
 350 is the total number of experimental data ($n = 251$).

351 The CCF value calculated with the original model prediction (with default parameters)
 352 was 83.46, but after the preliminary calibration step (optimization of PCCF) it was
 353 reduced to 67.68 (18.9% improvement).

354 The validation cost function (VCF) was calculated also with equation 5, but using
 355 experimental results of years 2008 to 2010.

356 Due to the associated uncertainty of full-scale WWTP, operational variables, as the
 357 plant flow rates and the DO in the aerobic basins could also be used as parameters to
 358 calibrate. The internal recycle, external recycle and purge flow rates data observed by
 359 the WWTP personnel probably contain uncertainties (no reliable flowmeters are usually
 360 available) and hence, some multiplying factors were created to consider these
 361 uncertainties. These factors were f_{QW} for the purge flow rate, f_{QRINT} for the internal
 362 recycle flow rate and f_{QRAS} for the external flow rate. In the case of the uncertainties of
 363 the DO sensors, the multiplying factor was the DO_Gain .

364 As the influent concentrations of each model variable neither are perfectly determined,
 365 additional influent factors were adopted for further adjustments in the inlet
 366 concentration of these variables.

367

368 **3.3 Parameter grouping for dynamic calibration**

369 The full plant model has about 90 model parameters, but only the 24 most sensitive
 370 parameters were studied. This set of 24 parameters was divided into three subsets: the

371 kinetic/stoichiometric parameters (group K, with 10 parameters), the influent
372 parameters (group I, with 10 parameters) and the operational parameters (group O, with
373 4 parameters). In fact, only parameters of the kinetic/stoichiometric macro-group were
374 used for real model calibration. The macro-groups I and O were used to obtain
375 additional information for process control and data quality.

376 The subset of kinetic/stoichiometric parameters was made up of the growth and decay
377 parameters, yields and saturation constants of all the involved biomasses (autotrophic,
378 heterotrophic and PAO). When calibrating the model with this group, it was assumed
379 that the influent composition during all the calibration period was completely known, as
380 well as the operational parameters. This assumption was not strictly correct since on-
381 line measurements of all the ASM2d states are never available. On the other hand, using
382 the subset of influent parameters, it was assumed that all the default
383 kinetic/stoichiometric ASM2d parameters were perfectly correct, as well as the
384 operational parameters. As determining on-line all the ASM2d variables in the influent
385 stream would be a very difficult and expensive task, the group I calibration was used for
386 obtaining additional information about the influent data quality and to determine which
387 variables in the influent could be easily modified in order to adjust the model. At last,
388 using the group of operational parameters, both kinetic/stoichiometric parameters and
389 the influent composition were considered perfectly fitting the biological processes rates
390 and the incoming pollutant loads, respectively. Amongst all the parameters, group O
391 was used for process control in the normal plant operation. Therefore, it was determined
392 the parameters of this group that more easily provided fast plant response to reject
393 external disturbances to the control system. This knowledge was obtained using the
394 same calibration methodology of the group K to the group O.

395

396 **3.4 Sensitivity Analysis**

397 Table 2 presents the overall sensitivity, calculated as the sum of relative sensitivity for
398 ammonium, phosphate, nitrate, TKN and TSS in the effluent (see the equations used in
399 the supplementary information S2). The advantage of using the relative sensitivity for
400 calculating the overall sensitivity is that all the output variables have the same
401 importance.

402 The parameters of each macro-group that most affect the model outputs were ranked in
403 descending order in this table. In the case of the K group, the heterotrophic biomass
404 growth yield, the nitrification and the phosphorus chemical precipitation are well
405 represented by the ranked parameters. K_{PRE} and K_{RED} have almost the same impact on
406 the model outputs, but their impacts are less important than the N removal processes.

407 Regarding the influent group, the inlet X_S , P-related processes and the inlet ammonium
408 concentration were the most important calibrating parameters. It is observed that PO_4^{3-}
409 or MeOH inlet concentrations are more important than the own kinetic precipitation
410 parameters K_{PRE} and K_{RED} of K group. These results indicate that chemical
411 P-precipitation and P-redissolution processes are kinetically limited due to the low
412 phosphate and MeOH concentration in the biological reactors.

413 In the case of the operational parameters, the purge flow rate and the DO have the most
414 influence on the model outputs. Nevertheless, all the parameters of this group would
415 have to change considerably to affect the outputs in the same quantity as the
416 kinetic/stoichiometric or the influent parameters. Table 2 also shows that inlet MeOH
417 concentration, which could be used to control P chemical precipitation, produces more
418 impact on the outputs than the process control variables considered in group O.
419 Regarding S_F inlet concentration, which could be used for controlling denitrification, it

420 would affect the outputs in the same extent of the best parameter of the group O, the
421 purge flow rate.

422 The previous sensitivity analysis was used to select the possible calibration parameters
423 for applying the “seeds” methodology. The K group has 10 elements that most affect the
424 model outputs. No more kinetic or stoichiometric parameters were included since the
425 10th parameter of the sensitivity list (Table 2) of this group ($\eta_{\text{NO}_3,\text{D}}$) only affects the
426 model output less than 10% the 1st parameter. The I group has all the influent states that
427 commonly could affect the model output. It is important to remember that this group
428 could be of size 19, the 19 state variables of the ASM2d, but the results of Table 2 show
429 that only the first nine affected the outputs. Finally, the O group has all the 4 variables
430 that are commonly used to control de WWTP processes. In case of adding external
431 readily organic matter to improve denitrification or phosphorus removal, such group of
432 parameters would have size of 5.

433

434 **3.5 Dynamic calibration methodology**

435 Dynamic calibration was performed following the methodology of the “seeds” [11] and
436 starting from the results obtained by the preliminary calibration and the sensitivity
437 analysis. This is the first reported application of this method using full-scale plant data.
438 The procedure uses the RDE criteria calculated from the Fisher Information Matrix
439 (FIM) as the ratio of normalized D to modified E criteria (RDE). From the sensitivity
440 ranking, the best-ranked parameters are named as “seeds”, since each one serves for
441 growing a parameter subset for model calibration. The subset generation process adds to
442 the seed subset a parameter that presents the highest RDE among the combination
443 between the current seed subset and all the other remaining best-ranked parameters of
444 the sensitivity rank. The process of generation of parameter subsets is automated,

445 independent of the user and exclusively based on mathematical tools, which was
446 considered a necessary improvement of model calibration techniques pointed out by Sin
447 et al. [18]. The “seed” methodology allows generating subsets with the maximum
448 capacity to explain plant behaviour with the less possible correlation amongst its
449 parameters. All the subsets generated could systematically be compared with each other.
450 The process of parameter addition repeats until the RDE decreases from the current
451 iteration to the previous one, for each seed. After that, the subset with the highest RDE
452 criterion is elected and the parameters values are already changed to the calibrated
453 values during the “seed” growth.

454

455 **3.6 Dynamic calibration results**

456 Tables 3, 4 and 5 present the results of applying the abovementioned calibration
457 methodology using parameters of groups K, I and O, respectively.

458

459 **3.6.1 Calibration of kinetic parameters**

460 The 10 best subsets were selected from the tested seeds. See Table 3 for details. The
461 common subset size is of 4 parameters. Nevertheless the highest RDE value was
462 calculated for a subset of 6 parameters (subset of seed $\eta_{NO_3,D}$). This subset produces the
463 lowest CCF and VCF, resulting in the most suitable subset for model calibration even
464 though the confidence interval of one parameter is considerably high. As the current
465 plant is an A/O WWTP, no parameters related to the biological P-removal appear in the
466 10 most impacting seeds. On the other hand, in all the subsets appears K_{PRE} or K_{RED} ,
467 parameters linked to the P-chemical precipitation. Y_H and b_H are present in all the
468 subsets, with high values of parameter confidence interval, which indicate less reliable
469 calibrating values. Parameter $\eta_{NO_3,D}$ is the parameter that provides more information

470 about the plant behaviour (lowest CCF and VCF when this parameter is inside the
471 calibration set), despite its lower value (0.0296) and more than 50% of confidence
472 interval (default ASM2d value is 0.80). Such value indicates that a poor denitrification
473 process is occurring in the plant caused by a lack of carbon source and some amount of
474 DO transported from the aerobic zone to the anoxic one. It would be recommendable to
475 add extra carbon source to the influent stream to increase the efficiency of the nitrogen
476 removal processes.

477 Considering that the influent composition determined by lab test and using plant data is
478 perfectly known along the years of calibration and validation data, the best subset
479 obtained following the methodology of Machado et al. [11] amongst the kinetic group is
480 the subset obtained from the parameter $\eta_{NO_3,D}$. The full subset is composed by the
481 parameters $\{\eta_{NO_3,D}, K_{PRE}, b_A, Y_H, K_{O_2,A}, b_H\}$ with values [0.0296, 1.005, 0.2203, 0.4181,
482 0.1130, 0.0829]. See Figure 4 for comparisons between the model prediction and the
483 plant data. In this subset, a calibrated value of 0.4181 for Y_H means that more COD is
484 consumed for maintenance of the heterotrophic biomass than the consumed for
485 promoting the growth of the microorganisms. It was not expected this low value for this
486 parameter, since the default value of Y_H is 0.625 [5]. However, similar values for Y_H
487 around 0.45 were obtained in the other subsets from the rest of seeds. Such an
488 unexpected result, probably, is derived from a lack of knowledge on the influent
489 composition and from the optimized values for sedimentation parameters obtained in
490 the static calibration. Nevertheless, $\eta_{NO_3,D}$ subset showed the best compromise between
491 explaining the plant behaviour and avoiding parameters correlations, with lower CCF
492 and VCF values.

493 Gross modelling errors could be corrected in the preliminary calibration step.
494 Nevertheless, poor BOD5 and ammonium predictions in the effluent could be an

495 indication that a false denitrification rate is occurring, probably because a lack of easily
496 biodegradable COD is not being captured. Figure 5 compares the model predictions to
497 the validation data, which is a completely different dataset from the calibration data. In
498 Figure 5, the parameters subset of the best seed of Table 3 makes the model suitable for
499 predicting correctly nitrate, phosphate, solids, TKN and COD in the effluent stream and
500 the solids in Q_{RAS} stream and inside the basins. The model predicts a very low
501 ammonium and BOD5 concentration in the effluent. Such results also could indicate
502 dead volumes in aerobic basins not modelled as well as a spatial gradient of DO,
503 ignored in the current model. As a consequence, not all the regions of the aerobic basins
504 operate with a reasonable DO concentration (2-3 mg/L). Figures 4 and 5 clearly show
505 that events with fast dynamics are not well captured, since some plant measurements
506 that made up calibration and validation data subsets have their sample time equal to one
507 day and the samples are integrated (each 2 hours a volume of wastewater is hold to
508 compose a final sample before chemical and biochemical analysis). Besides, the plant
509 data presents abrupt changes which bring additional difficulty to estimate model
510 parameter errors.

511

512 **3.6.2 Calibration of influent parameters**

513 Although the parameters of the influent group would not be used to make a real fit of
514 the model as in a conventional calibration procedure, some useful information can be
515 extracted from these results (Table 4). The optimized values of parameters are factors
516 that multiply the influent vectors for each variable of the influent. Therefore, a value of
517 1.414 of f_{SNH4} of the f_{SI} seed means that the ammonium vector of original plant data
518 increased 41.4% in order to minimize the cost function.

519 The most common subset size is 5 or 6 parameters. Parameters f_{SALK} , f_{XMeOH} , f_{SNH4} and
520 f_{SPO4} are present in almost all the subsets, which indicate that each variable is explaining
521 the model and is not interdependent amongst all of them. This information is also useful
522 to decide the influent variables where the sampling and measuring efforts should be
523 focused for a reliable optimization of kinetic parameters.

524 Table 4 also brings some other relevant remarks. The influent parameter group could
525 achieve good values of CCF and VCF in most of the tested subsets compared to the
526 subsets of the kinetic group. Thereby, if the weight of the influent parameter group (new
527 approach) is stronger than the kinetic one (traditional way) on the model prediction, the
528 variability of the influent composition and the error concerned to the characterization
529 procedure could explain the deviation between the current model and the standard
530 model ASM2d predictions. Therefore, these results demonstrate that the confidence of
531 the influent characterization is a key factor to consider before fitting any parameter of a
532 given model. In this sense, the importance of uncertainties associated to the influent
533 characterization that induce significant uncertainty in the model predictions have been
534 already highlighted in the literature [27, 28].

535 Comparing the results of f_{XTSS} and f_{XS} seeds it is observed that the result of f_{XTSS} seed
536 explains better the outputs than the result of f_{XS} seed, although the inclusion of f_{SF} in the
537 former subset increases correlation among parameters. In addition, the calibrating
538 methodology did not allow the simultaneous presence of f_{XS} and f_{XTSS} in any calibration
539 subset, probably due to the high correlation between these variables.

540 Finally, nitrate data are correlated to the S_F data, since in both created subsets where
541 f_{SNO3} appears (seeds f_{SNO3} and f_{SI}), high parameter confidence interval values are
542 reported. The existence of such correlation is clearly realized in the subset created by
543 the f_{SNO3} seed, which is made up only by f_{SNO3} and f_{SF} .

544

545 **3.6.3 Calibration of operational variables**

546 Considering the operational variables, only two different subsets could be created (see
547 Table 5), which means that almost all the variables help to explain the experimental
548 observations without correlation. Nevertheless, when inserting the biomass recycle flow
549 rate (f_{QRAS}) into a parameter calibration subset, a strong correlation to the internal
550 recycle flow rate was added. It indicates that in a possible control structure for
551 controlling simultaneously N, P and COD removal, the biomass recycle flow rate and
552 the internal recycle flow rate could not be changed at the same time or their
553 modifications should be done in different magnitudes to avoid its interaction.

554 Table 5 also shows that operational variables could improve model fit, i.e., the observed
555 variability with respect ASM2d prediction with default parameters could be explained
556 considering that the operational variables were not well measured. This is an important
557 problem in any model fit using full-scale WWTP data, where there are gradients and
558 time variability of operational variables, which do not have the same homogeneity and
559 reliability than in a controlled pilot WWTP.

560

561 **3.7 Remarks**

562 The “seeds” methodology applied to different group of parameters, not only the
563 traditional kinetic and stoichiometric ones, is a novel approach and allows:

- 564 • To automate the parameter subset selection, an improvement in the model
565 calibration techniques, pointed out by Sin et al. [18]. The usage of the sensitivity
566 analysis is similar to that found in BIOMATH protocol [21]. The “seed”
567 methodology searches for the minimal number of parameters that explains the
568 plant data with the less possible correlation amongst the calibration parameters.

569 The utilization of a higher number of parameters as in other works [24, 36]
570 provides a good model fit, but it is not usually supported by a study of its
571 correlation, which weakens its mathematical validity, as it is likely disregarding
572 overfitting problems that could reduce the model predictive capacity.

573 • To measure, in some extent, the influent states with higher uncertainties, which
574 aid to concentrate efforts in programming specific experiments to better
575 characterize these input variables (load disturbances). Such an uncertainty
576 measurement is in agreement to the philosophy of BIOMATH [21], STOWA
577 [20] and WERF [22] protocols, which are supported, amongst other premises, on
578 an excellent influent characterization.

579 • To identify the most correlated operational variables not to add them together
580 inside a control structure with decentralized controllers (e.g. PID controllers), to
581 avoid internal conflicts with the different control loops. Also, observing the CCF
582 and the confidence intervals of the best subsets of K and O groups, it is possible
583 to infer if some control structure designed based on the group O will be able to
584 compensate kinetic/stoichiometric uncertainties, since the industrial controllers
585 are model-based controllers, which means that the controllers performance are
586 dependent of the model accuracy. In the studied case, the operational variables
587 of Manresa WWTP are able to keep the plant under a stable operating point
588 since the CCF of subsets of the O group are lower than the K group as well as
589 the confidence intervals.

590

591 **4. Conclusions**

592 The ASM2d model was calibrated for the Manresa WWTP (Catalonia, Spain) using the
593 “seeds” methodology, which permits to calibrate models with the lowest number of

594 parameters, avoiding the correlation among the parameters optimized. As a novel
595 approach in ASM model calibration, the uncertainty on the influent characterization
596 could be evaluated fixing the kinetic and operational variables at their default/common
597 values and varying multipliers of the influent vector until reach the best objective
598 function value and lower correlation amongst the calibration parameters (multipliers).
599 One of the advantages of this novel approach was to identify what influent states should
600 be better characterized. In terms of process control, the applied methodology was able
601 to identify the most correlated operational variables, aiding to build decentralized
602 control structures with less internal conflicts amongst all the WWTP feedback loops.

603

604 **5. Acknowledgements**

605 The authors greatly acknowledge to Ricard Tomas and Ana Lupón (Aigües de Manresa
606 S.A.) all the support provided in conducting this work. Vinicius Cunha Machado has
607 received a Pre-doctoral scholarship of the AGAUR (Agència de Gestió d'Ajuts
608 Universitaris i Recerca - Catalonia, Spain), inside programs of the European
609 Community Social Fund. This work was supported by the Spanish Ministerio de
610 Economía y Competitividad (CTM2010-20384). The authors are members of the
611 GENOCOV research group (Grup de Recerca Consolidat de la Generalitat de
612 Catalunya, 2009 SGR 815).

613

614 **6. References**

- 615 1. Jeppsson U (1996) Modelling Aspects of Wastewater Treatment Processes. PhD
616 thesis. Available from <http://www.iea.lth.se/publications>. Lund Institute of
617 Technology, Sweden
- 618 2. Yuan Z, Bogaert H, Leten J, Verstraete W (2000) Reducing the size of a nitrogen
619 removal activated sludge plant by shortening the retention time of inert solids via
620 sludge storage. *Water Res* 34:539–549

- 621 3. Henze M, Grady Jr. CPL, Gujer W, Marais GR, Matsuo T (1987) Activated
622 sludge model No. 1, IAWQ Scientific and technical report No.1. IWAQ, London
- 623 4. Meijer SCF, van Loosdrecht MCM, Heijnen JJ (2002) Modelling the start-up of a
624 full-scale biological phosphorous and nitrogen removing WWTP. *Water Res*
625 36:4667–4682
- 626 5. Henze M, Gujer W, Mino T, van Loosdrecht MCM (2000) Activated sludge
627 models ASM1, ASM2, ASM2d and ASM3: Scientific and technical report No. 9.
628 IWA Publishing, London
- 629 6. Trutnau M, Petzold M, Mehlig L, Eschenhagen M, Geipel K, Müller S, Bley T,
630 Röske I (2011) Using a carbon-based ASM3 EAWAG Bio-P for modelling the
631 enhanced biological phosphorus removal in anaerobic/aerobic activated sludge
632 systems. *Bioprocess Biosyst Eng* 34:287–295
- 633 7. Ferrer J, Morenilla JJ, Bouzas A, García-Usach F (2004) Calibration and
634 simulation of two large wastewater treatment plants operated for nutrient
635 removal. *Water Sci Technol* 50:87–94
- 636 8. Ingildsen P, Rosen C, Gernaey KV, Nielsen MK, Guildal T, Jacobsen BN (2006)
637 Modelling and control strategy testing of biological and chemical phosphorus
638 removal at Avedøre WWTP. *Water Sci Technol* 53:105–113
- 639 9. Xie W-M, Zhang R, Li W-W, Ni B-J, Fang F, Sheng G-P, Yu H-Q, Song J, Le
640 D-Z, Bi X-J, Liu C-Q, Yang M (2011) Simulation and optimization of a full-
641 scale Carrousel oxidation ditch plant for municipal wastewater treatment.
642 *Biochem Eng J* 56:9–16
- 643 10. García-Usach F, Ferrer J, Bouzas A, Seco A (2006) Calibration and simulation of
644 ASM2d at different temperatures in a phosphorus removal pilot plant. *Water Sci*
645 *Technol* 53:199–206
- 646 11. Machado VC, Tapia G, Gabriel D, Lafuente J, Baeza JA (2009) Systematic
647 identifiability study based on the Fisher Information Matrix for reducing the
648 number of parameters calibration of an activated sludge model. *Environ Model*
649 *Softw* 24:1274–1284
- 650 12. Olsson G (2006) Instrumentation, control and automation in the water industry--
651 state-of-the-art and new challenges. *Water Sci Technol* 53:1–16
- 652 13. Copp JB, Spanjers H, Vanrolleghem PA (2002) *Respirometry in Control of the*
653 *Activated Sludge Process: Benchmarking Control Strategies*. Scientific and
654 Technical Report N° 11. 160
- 655 14. Vrecko D, Hvala N, Stare A, Burica O, Strazar M, Levstek M, Cerar P,
656 Podbevsek S (2006) Improvement of ammonia removal in activated sludge
657 process with feedforward-feedback aeration controllers. *Water Sci Technol*
658 53:125–132

- 659 15. Samuelsson P, Carlsson B (2001) Feed-forward control of the external carbon
660 flow rate in an activated sludge process. *Water Sci Technol* 43:115–122
- 661 16. Ayesa E, De La Sota A, Grau P, Sagarna JM, Salterain A, Suescun J (2006)
662 Supervisory control strategies for the new WWTP of Galindo-Bilbao: the long
663 run from the conceptual design to the full-scale experimental validation. *Water*
664 *Sci Technol* 53:193–201
- 665 17. Orhon D, Artan N, Ates E (1994) A description of three methods for the
666 determination of the initial inert particulate chemical oxygen demand of
667 wastewater. *J Chem Technol Biotechnol* 61:73–80
- 668 18. Sin G, Van Hulle SWH, De Pauw DJW, van Griensven A, Vanrolleghem PA
669 (2005) A critical comparison of systematic calibration protocols for activated
670 sludge models: a SWOT analysis. *Water Res* 39:2459–2474
- 671 19. Ruano M V, Ribes J, De Pauw DJW, Sin G (2007) Parameter subset selection for
672 the dynamic calibration of activated sludge models (ASMs): experience versus
673 systems analysis. *Water Sci Technol* 56:107–115
- 674 20. Hulsbeek JJW, Kruit J, Roeleveld PJ, van Loosdrecht MCM (2002) A practical
675 protocol for dynamic modelling of activated sludge systems. *Water Sci Technol*
676 45:127–136
- 677 21. Vanrolleghem PA, Insel G, Petersen B, Sin G, De Pauw D, Nopens I, Dovermann
678 H, Weijers S, Gernaey K (2003) A comprehensive model calibration procedure
679 for activated sludge. WEFTEC 76th Annu. Tech. Exhib. Conf. Water
680 Environment Federation, Los Angeles, California, pp 210–237
- 681 22. Melcer H, Dold PL, Jones RM, Bye CM, Takacs I, Stensel HD, Wilson AW, Sun
682 P, Bury S (2003) *Methods for Wastewater Characterization in Activated Sludge*
683 *Modelling*. Water Environment Research Foundation (WERF), Alexandria, VA,
684 USA
- 685 23. Langergraber G, Rieger L, Winkler S, Alex J, Wiese J, Owerdieck C, Ahnert M,
686 Simon J, Maurer M (2004) A guideline for simulation studies of wastewater
687 treatment plants. *Water Sci Technol* 50:131–138
- 688 24. Cosenza A, Mannina G, Neumann MB, Viviani G, Vanrolleghem PA (2013)
689 Biological nitrogen and phosphorus removal in membrane bioreactors: model
690 development and parameter estimation. *Bioprocess Biosyst Eng* 36:499–514
- 691 25. Mannina G, Cosenza A, Vanrolleghem PA, Viviani G (2011) A practical
692 protocol for calibration of nutrient removal wastewater treatment models. *J*
693 *Hydroinformatics* 13:575–595
- 694 26. Refsgaard JC, van der Sluijs JP, Højberg AL, Vanrolleghem PA (2007)
695 Uncertainty in the environmental modelling process – A framework and
696 guidance. *Environ Model Softw* 22:1543–1556

- 697 27. Sin G, Gernaey K V, Neumann MB, Van Loosdrecht MCM, Gujer W (2009)
698 Uncertainty analysis in WWTP model applications: a critical discussion using an
699 example from design. *Water Res* 43:2894–2906
- 700 28. Cierkens K, Plano S, Benedetti L, Weijers S, de Jonge J, Nopens I (2012) Impact
701 of influent data frequency and model structure on the quality of WWTP model
702 calibration and uncertainty. *Water Sci Technol* 65:233–242
- 703 29. Mannina G, Cosenza A, Viviani G (2012) Uncertainty assessment of a model for
704 biological nitrogen and phosphorus removal: Application to a large wastewater
705 treatment plant. *Phys Chem Earth, Parts A/B/C* 42-44:61–69
- 706 30. Benedetti L, Batstone DJ, De Baets B, Nopens I, Vanrolleghem PA (2012)
707 Uncertainty analysis of WWTP control strategies made feasible. *Water Qual Res*
708 *J Canada* 47:14
- 709 31. Belia E, Amerlinck Y, Benedetti L, Johnson B, Sin G, Vanrolleghem PA,
710 Gernaey K V, Gillot S, Neumann MB, Rieger L, Shaw A, Villez K (2009)
711 Wastewater treatment modelling: dealing with uncertainties. *Water Sci Technol*
712 60:1929–1941
- 713 32. Takács I, Patry GG, Nolasco D (1991) A dynamic model of the clarification-
714 thickening process. *Water Res* 25:1263–1271
- 715 33. Orhon D, Artan N (1994) Modelling of activated sludge systems. 589p
- 716 34. Montpart N (2010) Redesign of a Dissolved Oxygen Control System in an Urban
717 WWTP. Master in Environmental Studies. Universitat Autònoma de Barcelona,
718 Barcelona, Catalonia, Spain.
- 719 35. Sin G, Gernaey K V, Neumann MB, Van Loosdrecht MCM, Gujer W (2009)
720 Uncertainty analysis in WWTP model applications: a critical discussion using an
721 example from design. *Water Res* 43:2894–2906
- 722 36. Vangsgaard AK, Mutlu AG, Gernaey K V, Smets BF, Sin G (2013) Calibration
723 and validation of a model describing complete autotrophic nitrogen removal in a
724 granular SBR system. *J Chem Technol Biotechnol* 88:2007–2015
- 725
- 726

727

728 **Fig. 1** Scale map of the Manresa WWTP

729

730 **Fig. 2** Monitored variables of the Manresa WWTP secondary treatment

731

732 **Fig. 3** Simplified scheme of the overall calibration / validation process

733

734 **Fig. 4** Model predictions using the best seed (subset from the seed $\eta_{\text{NO}_3,\text{D}}$) and plant data

735 (calibration data). For checking the parameter values used in this simulation, see Table

736 3

737

738 **Fig. 5** Model predictions using the best subset (from seed $\eta_{\text{NO}_3,\text{D}}$) and the validation data

739 (plant data)

740

741

742

743

744 **Table 1:** Average influent composition.

Property	Winter (Average Temperature = 13°C)	Summer (Average Temperature = 27°C)
pH	7.9	7.6
NH₄⁺ [mg N/L]	33	20
BOD5 [mg/L]	290	170
COD [mg/L]	600	460
Total N [mg N/L]	53	33
NO₃⁻ [mg N/L]	3.5	2.0
Total P, [mg P/L]	8.0	5.5
TKN [mg N/L] (Kjeldahl nitrogen)	48	33
Zn [mg Zn/L]	0.8	0.5

745

746

747

748

749

750

751 **Table 2:** Relative sensitivity of the weighted sum of ammonium, phosphate, nitrate,

752 TKN and TSS in the effluent, for all the three groups of parameters.

Kinetic / Stoichiometric Group (K group)				
Order	Parameter	Short Description	Related biomass or process	Sensitivity
1	Y_H	Yield coefficient for X_H .	Heterotrophic	756
2	μ_A	Maximum growth rate of X_A	Autotrophic	678
3	b_A	Rate for lysis of X_A	Autotrophic	634
4	$K_{NH_4,A}$	Saturation coefficient of substrate NH_4^+ for nitrification on S_{NH_4}	Autotrophic	412
5	K_{PRE}	Precipitation constant	Chemical phosphate precipitation	150
6	$K_{O_2,A}$	Saturation coefficient of O_2 for nitrification on S_{NH_4}	Autotrophic	149
7	K_{RED}	Solubilisation constant	Chemical phosphate precipitation	148
8	b_H	Rate for lysis of X_H	Heterotrophic	97
9	$K_{ALK,A}$	Saturation coefficient of alkalinity for nitrification on S_{NH_4}	Autotrophic	73
10	$\eta_{NO_3,D}$	Reduction factor for denitrification	Heterotrophic	51
Influent Group (I group)				
Order	Parameter	Short Description	Related biomass or process	Sensitivity
1	f_{X_S}	Multiplying factor of X_S representing an uncertainty on the estimated inlet X_S fraction	Influent characterization	670
2	$f_{X_{TSS}}$	Multiplying factor of the inlet X_{TSS} vector.	Influent characterization	555
3	$f_{X_{MeOH}}$	Multiplying factor of the inlet X_{MeOH} vector.	Influent characterization	439
4	$f_{S_{PO_4}}$	Multiplying factor of the inlet S_{PO_4} vector.	Influent	429

5	f_{SNH_4}	Multiplying factor of the inlet S_{NH_4} vector.	Influent characterization	393
6	f_{SF}	Multiplying factor of the inlet S_{F} vector.	Influent characterization	247
7	f_{SALK}	Multiplying factor of the inlet S_{ALK} vector.	Influent characterization	169
8	f_{SI}	Multiplying factor of the inlet S_{I} vector.	Influent characterization	160
9	f_{SNO_3}	Multiplying factor of the inlet S_{NO_3} vector.	Influent characterization	87
10	f_{SA}	Multiplying factor of the inlet S_{A} vector.	Influent characterization	0
Operational Group (O group)				
Order	Parameter	Short Description	Related biomass or process	Sensitivity
1	f_{QW}	Multiplying factor of Q_{W} representing an uncertainty on the measured value of Q_{W} .	Process control	297
2	DO_Gain	Multiplying factor of DO concentration on the aerobic basins representing an uncertainty on the measured value of DO.	Process control	180
3	f_{QRINT}	Multiplying factor of Q_{RINT} representing an uncertainty on the measured value of Q_{RINT} .	Process control	135
4	f_{QRAS}	Multiplying factor of Q_{RAS} representing an uncertainty on the measured value of Q_{RAS} .	Process control	116

753

754

755

756

757 **Table 3:** Results of the calibration methodology for the kinetic Group K.

Items	Seeds									
	Y_H	μ_A	b_A	$K_{NH_4,A}$	K_{PRE}	$K_{O_2,A}$	K_{RED}	b_H	$K_{ALK,A}$	$\eta_{NO_3,D}$
Parameters	Y_H	μ_A	b_A	$K_{NH_4,A}$	K_{PRE}	$K_{O_2,A}$	K_{RED}	b_H	$K_{ALK,A}$	$\eta_{NO_3,D}$
	b_A	Y_H	Y_H	K_{PRE}	μ_A	K_{PRE}	μ_A	K_{RED}	K_{PRE}	b_A
	K_{PRE}	K_{PRE}	K_{PRE}	Y_H	Y_H	Y_H	Y_H	μ_A	Y_H	Y_H
	b_H	b_H	b_H	b_H	b_H	b_H	b_H	b_H	Y_H	b_H
										$K_{O_2,A}$
Optimized Values	0.452	0.908	0.168	1.616	1.013	0.089	0.593	0.101	0.895	1.005
	0.168	0.448	0.452	1.011	0.908	1.008	0.908	0.593	1.011	0.2203
	1.045	1.013	1.045	0.457	0.448	0.4105	0.448	0.908	0.449	0.4181
	0.104	0.102	0.104	0.108	0.102	0.0786	0.101	0.448	0.103	0.1130
						0.2277				0.0829
Parameter	22	3	3	6	9	68	9	66	16	9
Confidence	3	26	22	9	3	9	3	9	9	9
Interval	9	9	9	21	26	30	27	3	25	22
(%)	59	64	59	48	64	71	66	27	61	114
						5				52
Norm of Parameter										
Confidence	64	70	64	53	70	103	72	72	68	138
Interval										
(%)										
normD	$1.58 \cdot 10^{14}$	$4.72 \cdot 10^{12}$	$1.58 \cdot 10^{14}$	$5.46 \cdot 10^{11}$	$4.72 \cdot 10^{12}$	$1.81 \cdot 10^{16}$	$1.02 \cdot 10^{13}$	$1.02 \cdot 10^{13}$	$1.45 \cdot 10^{11}$	$9.40 \cdot 10^{21}$
modE	393.41	62.61	393.41	46.37	62.61	491.80	69.09	69.09	69.56	1420.93
RDEc	$4.03 \cdot 10^{11}$	$7.55 \cdot 10^{10}$	$4.03 \cdot 10^{11}$	$1.18 \cdot 10^{10}$	$7.55 \cdot 10^{10}$	$3.68 \cdot 10^{13}$	$1.47 \cdot 10^{11}$	$1.47 \cdot 10^{11}$	$2.09 \cdot 10^9$	$6.61 \cdot 10^{18}$
CCF	66.3	66.3	66.3	65.1	66.3	65.5	66.3	66.3	66.4	63.5
VCF	172.1	172.1	172.1	170.4	172.1	171.2	172.1	172.1	172.3	167.7
Janus	1.288	1.288	1.288	1.294	1.288	1.292	1.288	1.288	1.288	1.295

758

759

760

761

762

764 **Table 4:** Results of the calibration methodology for the Group I.

Items	Seeds										
	f _{XS}	f _{XTSS}	f _{XMeOH}	f _{SPO4}	f _{SNH4}	f _{SF}	f _{SALK}	f _{SI}	f _{SNO3}	f _{SA}	
Parameters								f _{SI}			
		f _{XTSS}				f _{SF}	f _{SALK}	f _{SPO4}			
	f _{XS}	f _{SF}	f _{XMeOH}	f _{SPO4}	f _{SNH4}	f _{XTSS}	f _{SF}	f _{SNH4}			
	f _{SNH4}	f _{SNH4}	f _{SNH4}	f _{SNH4}	f _{SPO4}	f _{SNH4}	f _{XTSS}	f _{SALK}	f _{SNO3}	-	
	f _{SPO4}	f _{SALK}	f _{SALK}	f _{SALK}	f _{SALK}	f _{SALK}	f _{SNH4}	f _{XS}	f _{SF}		
	f _{SALK}	f _{SPO4}	f _{XS}	f _{XS}	f _{XS}	f _{SPO4}	f _{SPO4}	f _{XMeOH}			
f _{XMeOH}	f _{XMeOH}	f _{SPO4}	f _{XMeOH}	f _{XMeOH}	f _{XMeOH}	f _{XMeOH}	f _{XMeOH}	f _{SF}			
Optimized Values								f _{SNO3}			
								6.835			
		0.537				2.861	1.126	0.706			
	1.038	2.861	0.936	0.758	1.116	0.537	2.861	1.414			
	1.116	1.433	1.116	1.116	0.758	1.433	0.537	1.266	1.009	-	
	0.758	1.126	0.949	0.949	0.949	1.126	1.433	1.361	0.929	-	
0.949	0.708	1.038	1.038	1.038	0.708	0.708	1.229				
0.936	1.223	0.758	0.936	0.936	1.223	1.223	2.472				
Parameter Confidence Interval (%)								0.144			
								7			
	9	26	10	10	4	16	6	12			
	4	16	4	4	10	26	16	5			
	10	5	6	6	6	5	26	13	35	-	
	6	6	9	9	9	6	5	912	9	-	
10	12	9	9	9	12	12	18				
	11	10	10	10	11	11	96				
Norm of Parameter Confidence Interval (%)											
	18	35	18	18	18	35	35	101	36	-	
	normD	$1.336 \cdot 10^1_6$	$2.635 \cdot 10^{16}$	$1.336 \cdot 10^{16}$	$1.336 \cdot 10^{16}$	$1.336 \cdot 10^{16}$	$2.635 \cdot 10^{16}$	$2.635 \cdot 10^{16}$	$9.148 \cdot 10^1_8$	16598	-
	modE	99.320	1480.73	99.320	99.320	99.320	1480.73	1480.73	1138.80	18.66	-
RDEc	$1.345 \cdot 10^1_4$	$1.779 \cdot 10^{13}$	$1.345 \cdot 10^{14}$	$1.345 \cdot 10^{14}$	$1.345 \cdot 10^{14}$	$1.779 \cdot 10^{13}$	$1.779 \cdot 10^{13}$	$8.033 \cdot 10^1_5$	889	-	
CCF	66.1	63.6	66.1	66.1	66.1	63.6	63.6	55.8	67.6	-	
VCF	170.9	168.4	170.8	170.8	170.8	168.4	168.4	162.3	172.3	-	
Janus	1.289	1.311	1.289	1.289	1.289	1.311	1.311	1.371	1.278	-	

767

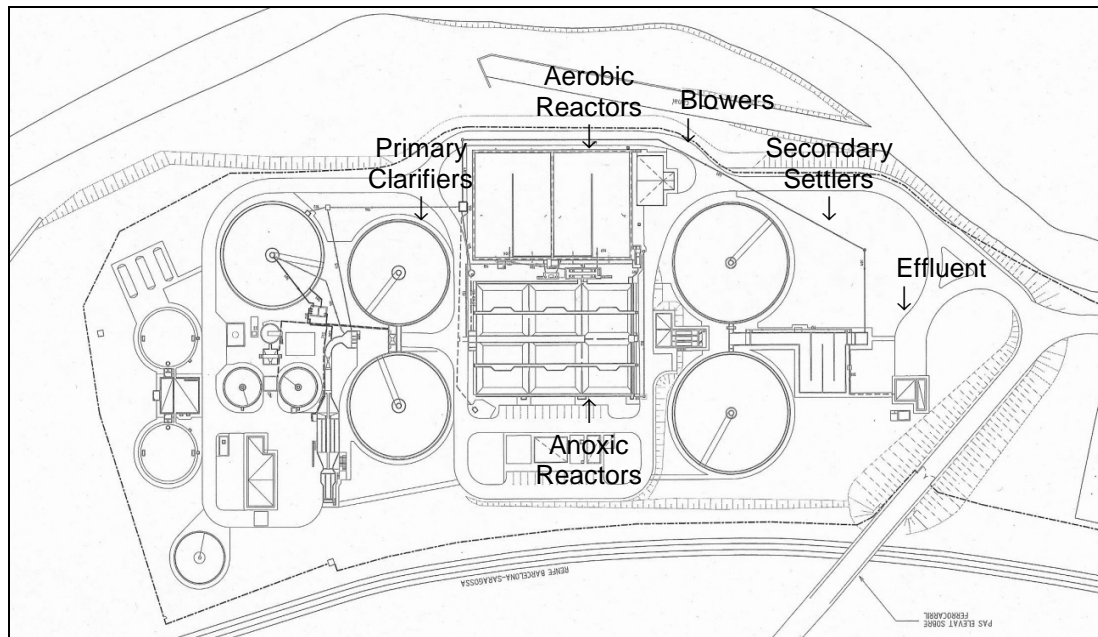
768 **Table 5:** Results of the calibration methodology for the Group O.

Items	Seeds			
	fQ _w	DO_Gain	fQ _{rint}	fQ _{RAS}
Parameters	fQ _w	DO_Gain	fQ _{rint}	fQ _{RAS}
	fQ _{rint}	fQ _w	fQ _w	DO_Gain
	DO_Gain	fQ _{rint}	DO_Gain	fQ _{rint}
				fQ _w
Optimized Values	0.344	0.931	0.389	2.781
	0.389	0.344	0.344	0.925
	0.931	0.389	0.931	0.122
				0.388
Parameter	8	11	18	15
Confidence	18	8	8	11
Interval (%)	11	18	11	97
Norm of Parameter Confidence Interval (%)				9
	23	22	22	99
normD	1.61·10 ⁹	1.61·10 ⁹	1.61·10 ⁹	3.26·10 ¹⁰
modE	13.78	13.78	13.78	193.77
RDEc	1.17·10 ⁸	1.17·10 ⁸	1.17·10 ⁸	1.680·10 ⁸
CCF	62.3	62.3	62.3	62.2
VCF	168.9	168.9	168.9	168.9
Janus	1.322	1.322	1.322	1.323

769

770

771



772

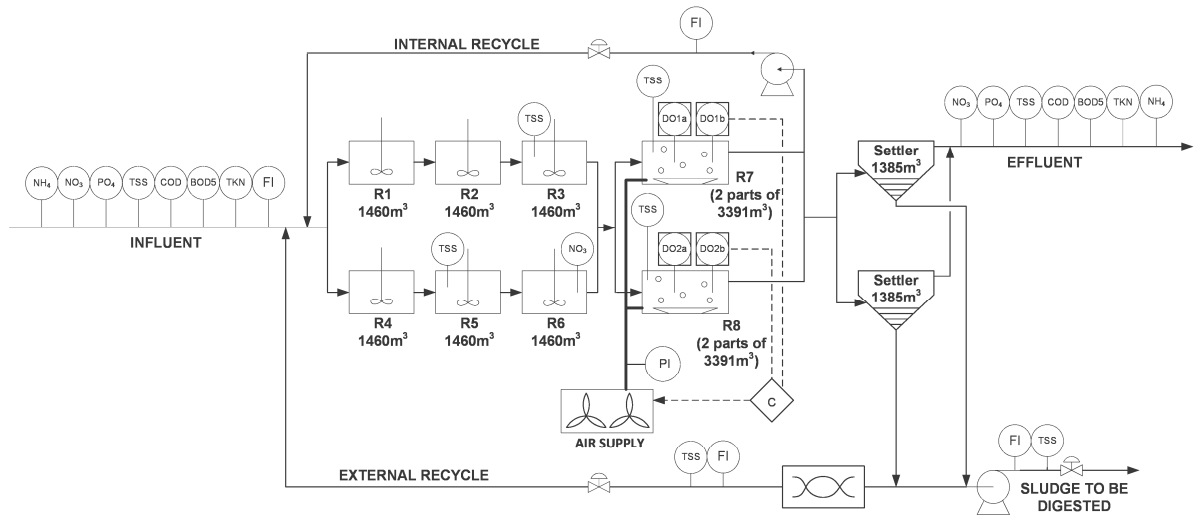
773 **Fig. 1** Scale map of the Manresa WWTP

774

775

776

777



778

779

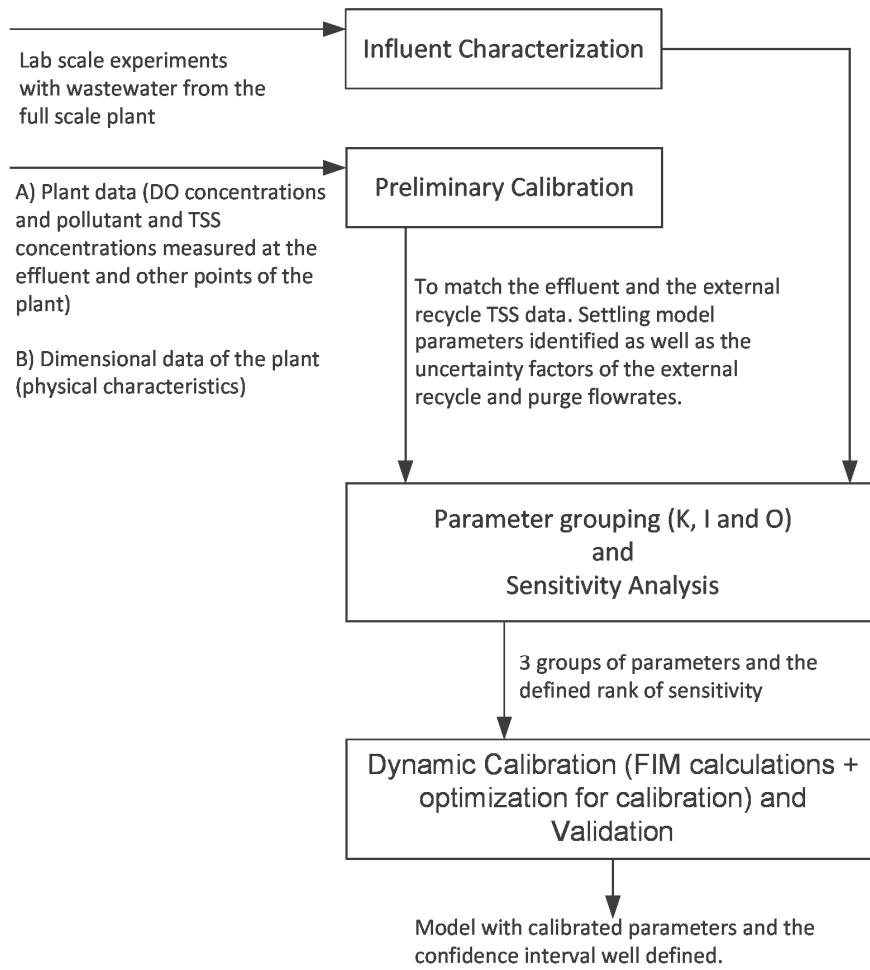
780 **Fig. 2** Monitored variables of the Manresa WWTP secondary treatment

781

782

783

784



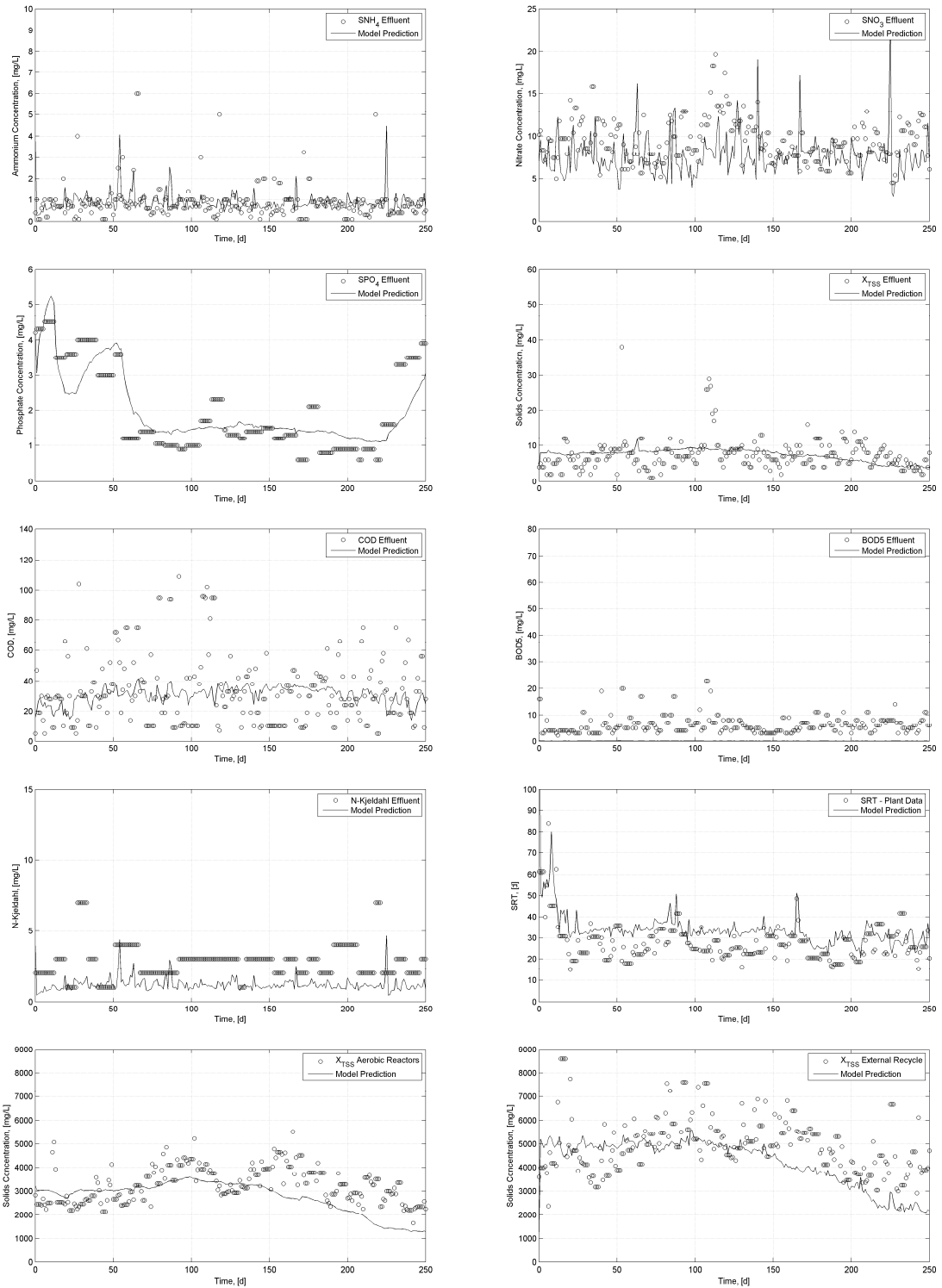
785

786

787 **Fig. 3** Simplified scheme of the overall calibration / validation process

788

789



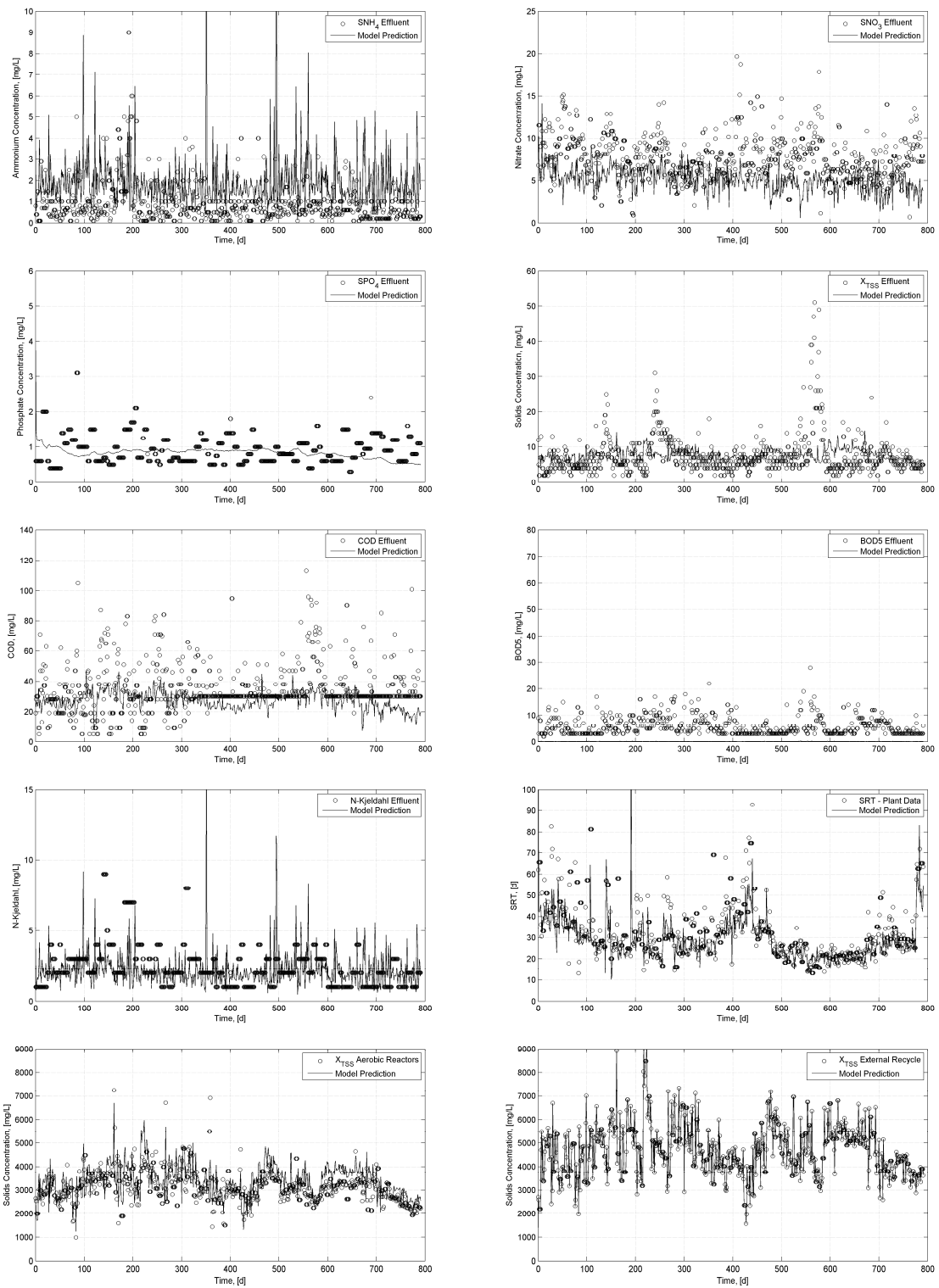
790

791 **Fig. 4** Model predictions using the best seed (subset from the seed $\eta_{NO_3,D}$) and plant data
 792 (calibration data). For checking the parameter values used in this simulation, see Table

793 3

794

795



796

797 **Fig. 5** Model predictions using the best subset (from seed $\eta_{NO3,D}$) and the validation data

798 (plant data)

799

800

801

Supplementary information

802

803 **Activated Sludge Model 2d calibration with full-scale WWTP data: comparing**
804 **model parameter identifiability with influent and operational uncertainty.**

805

806 Vinicius Cunha Machado, Javier Lafuente, Juan Antonio Baeza*

807

808 Department of Chemical Engineering, Universitat Autònoma de Barcelona, ETSE,

809 08193 Bellaterra (Barcelona), Spain. Phone: +34935811587. FAX: +34935812013.

810 E-mails: vinicius.cunhamachado@gmail.com, javier.lafuente@uab.cat,

811 juanantonio.baeza@uab.cat

812 *Corresponding Author

813

814 **S1. Influent Characterization Procedure**

815 Orhon *et al.* [1] developed a method to determine the values of S_I , X_I , X_S and S_F
816 (ASM2d states) in the effluent, using the well-know measurement of the COD. X
817 variables are the particulate variables while S variables indicate soluble variables. Such
818 method allows making an interface between the COD and ASM2d state variables.

819 The experimental determination of S_I and X_I is performed in two parallel CSTR reactors,
820 one of them fed with raw WWTP influent and the other one fed with filtered WWTP
821 influent. Both reactors operate as long as all the biological reactions have been ceased
822 and daily analysis of total COD and the soluble COD are performed. At a sufficient
823 time, both values of COD of the two systems will be approximately constant. At the end
824 of the experiment, the relationship between the initial and final values of total COD and
825 soluble COD of both systems will help to estimate S_I and X_I .

826 X_S is present at the beginning of the experiment for reactor 1 (with raw influent, without
827 filtering) and it is not for reactor 2 (with filtered WW). At the end of the experiment, in
828 both systems X_S and S_F no longer exist, differently of S_P and X_P that are produced by the
829 microorganisms along the experiment time. S_P and X_P are, respectively, soluble and
830 particulate residual biodegradable matter, product of microorganism activity. X_I is
831 present at the end of the experiment only in reactor 1 (no filtered WW). With these
832 observations, it is possible to write a system of equations as follows:

833

834

Reactor 1 (Fed with raw wastewater)	Reactor 2 (Fed with filtered wastewater)
$C_{T0} = S_{F0} + X_{S0}$ Eq. S.1	$C_{T0} = S_{T0}$ Eq. S.4
$C_{T1} = X_{I1} + S_{I1} + X_{P1} + S_{P1}$ Eq. S.2	$C_{T2} = X_{I2} + S_{I2} + X_{P2} + S_{P2}$ Eq. S.5
$S_{T1} = S_{I1} + S_{P1}$ Eq. S.3	$S_{T2} = S_{I2} + S_{P2}$ Eq. S.6

835

836 Variable C_T means the total substrate concentration in reactors. S_T means total soluble
 837 substrate. The lowercase “0” in equations S.1 and S.4 means “initial value” for variables
 838 in reactor 1 and 2, respectively. In equations S.2 and S.3 the lowercase “1” means the
 839 values at the end of the experiment in reactor 1. The same notation is used for reactor 2,
 840 in equations S.5 and S.6. For a better understanding of the whole experiment, Figure S.1
 841 shows an illustration of the evolution of total COD and total soluble COD.

842 Using the equations S.1 to S.6, X_I is determined with equation S.7.

843

$$844 \quad X_I = (C_{T1} - S_{T1}) - \left\{ [C_{T2} - S_{T2}] \cdot \frac{[C_{T0} - C_{T1}]}{[S_{T0} - C_{T2}]} \right\} \quad \text{Eq. S.7}$$

845

846 A similar procedure is performed to determine S_I .

847

$$848 \quad S_I = S_{T1} - \left\{ \frac{S_{T1} - S_{T2}}{1 - \left[\frac{S_{T0} - C_{T2}}{C_{T0} - C_{T1}} \right]} \right\} \quad \text{Eq. S.8}$$

849 S_F value can be obtained by taking the value of total soluble COD of reactor 2 at the
 850 beginning of the experiment for determining X_I and S_I and subtracting the value of S_I
 851 (obtained by Eq. S.8).

852

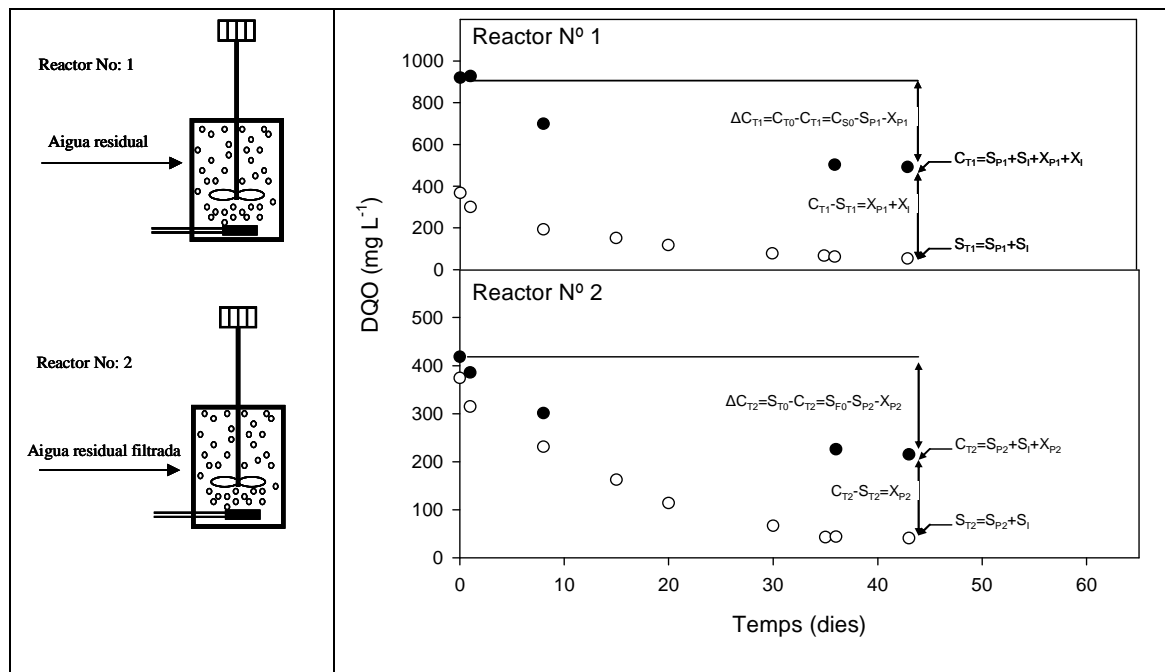
$$853 \quad S_F = COD_{\text{Soluble (filtered WW)}} - S_I \quad \text{Eq. S.9}$$

854 Finally, X_S is determined by using measures of total COD in reactor 1.

$$855 \quad X_S = DQO_{\text{total}} - (S_A + S_F + S_I + X_I) \quad \text{Eq. S.10}$$

856 In Eq. S.10, S_A should be considered null (no conditions of fermenting X_S to produce S_A
 857 in the urban sewage system) and the rest of variables were already determined.

858



859 **Figure S.1:** Illustration of the lab scale reactors, total COD and total soluble COD data
 860 for determining S_I and X_I fractions in the secondary stage influent in a WWTP
 861 (• Total COD, ○ Total soluble COD).

862

863 S.2. Sensitivity Analysis

864 Sensitivity analysis allows making a ranking of the most important parameters that
865 affect the outputs. Relative sensitivity of an output i (y_i) respect a parameter j (θ_j) is
866 defined as [2],

$$867 \quad S_{ij} = \frac{\theta_j}{y_i} \frac{dy_i}{d\theta_j} \quad \text{Eq. S.11}$$

868 Norton [3] proposed the utilization of algebraic sensitivity analysis because the
869 numerical value of sensitivity applies only for a specific change from a specific value of
870 θ_j , while the former provides algebraic relations. Numerical values of sensitivity are
871 generally much less informative than an algebraic relation, but algebraic sensitivity
872 analysis is not feasible if the equations of the model are complicated as in ASM2d.
873 Therefore, the derivatives of equation S.11 were determined numerically by the finite
874 differences method. The central difference approach with 10^{-4} (0.01%) as perturbation
875 factor was used for the sensitivity calculations of each tested parameter around the
876 default ASM2d value. This perturbation factor was selected because it produced equal
877 derivative values with forward and backward finite differences [4].

878 The overall sensitivity of a parameter was calculated by adding absolute values of
879 individual sensitivities. In our case, 5 output variables were declared (phosphate,
880 ammonium, nitrate, TSS and TKN concentrations at the effluent). Hence, the overall
881 sensitivity value of a parameter j (OS_j) was calculated with equation S.12.

$$882 \quad OS_j = |S_{j,PO_4}| + |S_{j,NH_4}| + |S_{j,NO_3}| + |S_{j,XTSS}| + |S_{j,TKN}| \quad \text{Eq. S.12}$$

883

884

885

886 **S.3. The Fisher Information Matrix and Parameter Confidence Interval**

887 The FIM summarizes the importance of each model parameter over the outputs, since it
 888 measures the variation of output variables caused by a variation of model parameters [5,
 889 6]. Algebraically, the FIM is represented by equation S.13.

$$890 \quad FIM = \sum_{k=1}^N Y_{\theta}(k) \cdot Q_k^{-1} \cdot Y_{\theta}^T(k) \quad \text{Eq. S.13}$$

891 For a FIM calculated for r output variables and p parameters, it is a $p \times p$ matrix, where
 892 k represents each sampling data point, Q_k is the $r \times r$ covariance matrix of the
 893 measurement noise, θ is the vector of p parameters, N is the total number of samples
 894 and Y_{θ} is the $p \times r$ output sensitivity function matrix, expressed by equation S.14.

$$895 \quad Y_{\theta}^T(t) = \left[\frac{\partial y(t, \theta_0)}{\partial \theta^T} \right]_{\theta_0} \quad \text{Eq. S.14}$$

896 where θ_0 is the complete model parameter vector used for calculating the derivatives
 897 and θ_T is the transposed parameter vector, which its elements are being studied. In the
 898 present study, the derivative shown in equation S.14 was numerically obtained by finite
 899 differences using a perturbation factor of 10^{-4} as in the sensitivity calculations.
 900 Mathematically was proved that the FIM provides a lower bound of the parameter error
 901 covariance matrix [7] as shown by equation S.15.

$$902 \quad \text{cov}(\theta_0) \geq FIM^{-1} \quad \text{Eq. S.15}$$

903 This FIM property was used for calculating the confidence interval $\Delta\theta_j$ with equation
 904 S.16 for a given parameter θ_j [8].

$$905 \quad \Delta\theta_j = t_{\alpha, N-p} \sqrt{\text{cov}(\theta_j)} \quad \text{Eq. S.16}$$

906 where t is the statistical t-student with $\alpha = 95\%$ of confidence and $N-p$ degrees of
907 freedom (number of experimental data points minus p parameters), and $\text{cov}(\theta_j)$ was
908 assumed as FIM^{-1}_{jj} .

909 As can be observed, the calculation of the parameter error covariance matrix using the
910 FIM involves its inversion. To be invertible, the FIM should have a determinant
911 different from zero and should not be ill-conditioned. To match these requirements any
912 pair of matrix columns should not be very similar. As each column of the matrix
913 represents a parameter, the determinant and the condition number of the FIM provides a
914 reasonable measurement of the correlation of a set of parameters. Hence, parameters
915 less correlated will easily provide a diagonal-dominant matrix. The FIM determinant (D
916 criterion) and the ratio between the highest and the lowest FIM eigenvalue (modE
917 criterion) can be used as criteria for parameter subset selection. A modE criterion value
918 close to the unity indicates that all the involved parameters independently affect the
919 outputs while the shape of the confidence region is similar to a circle (2 parameters) or a
920 sphere (3 parameters) and not ellipses and ellipsoids as occur with correlated
921 parameters. A high D criterion value means lower values of the diagonal elements of the
922 covariance matrix, and as a consequence, lower confidence intervals of the parameters.
923 As the D criterion is dependent on the magnitude of the involved parameters, this
924 criterion was normalized (normD) according to Equation S.17.

$$925 \quad \text{normD} = D \cdot \|\theta_p\|^2 \quad \text{Eq. S.17}$$

926 where $\|\theta_p\|$ is the Euclidean norm of the parameter vector. Such normalization works as
927 a scaling factor and allows comparisons among subsets with the same size but with
928 different parameters.

929 From the system engineering point of view, it is important to include in the parameter
930 subset those parameters that maximize the D criterion and minimize the modE criterion.

931 Hence, the ratio between the normD and the modE criteria (RDE criterion) was
932 proposed [9] as an interesting index to define subsets of parameters for calibration. The
933 RDE criterion (Equation S.18) establishes the capacity of a parameter subset to explain
934 experimental data coupled to low uncertainty in the estimated parameters.

$$935 \quad RDE = \frac{normD}{modE} \quad \text{Eq. S.18}$$

936

937 **S.4. References**

- 938 1. Orhon D, Artan N, Ates E (1994) A description of three methods for the
939 determination of the initial inert particulate chemical oxygen demand of
940 wastewater. *J Chem Technol Biot* 61:73–80
- 941 2. Reichert P, Vanrolleghem PA (2001) Identifiability and uncertainty analysis of
942 the river water quality model no. 1 (RWQM1). *Water Sci Technol* 43:329–338
- 943 3. Norton JP (2008) Algebraic sensitivity analysis of environmental models.
944 *Environ Model Softw* 23:963–972
- 945 4. De Pauw DJW (2005) Optimal Experimental Design for Calibration of
946 Bioprocess Models: A Validated Software Toolbox. PhD thesis in Applied
947 Biological Sciences. Available from:
948 <http://biomath.ugent.be/publications/download/>. University of Gent, Belgium
- 949 5. Dochain D, Vanrolleghem PA (2001) Dynamical modelling and estimation in
950 wastewater treatment processes. IWA Publishing, London
- 951 6. Guisasola A, Baeza JA, Carrera J, Sin G, Vanrolleghem PA, Lafuente J (2006)
952 The influence of experimental data quality and quantity on parameter estimation
953 accuracy. *Education for Chemical Engineers* 1:139–145
- 954 7. Söderström T, Stoica P (1989) System identification. Prentice-Hall, Englewood
955 Cliffs, New Jersey
- 956 8. Seber GAF, Wild CJ (1989) Nonlinear regression. Wiley, New York
- 957 9. Machado VC, Tapia G, Gabriel D, Lafuente J, Baeza JA (2009) Systematic
958 identifiability study based on the Fisher Information Matrix for reducing the
959 number of parameters calibration of an activated sludge model. *Environ Model*
960 *Softw* 24:1274–1284

961